

Eye Gaze-Informed and Context-Aware Pedestrian Trajectory Prediction in Shared Spaces with Automated Shuttles: A Virtual Reality Study

Danya Li, Yan Feng, Rico Krueger

Abstract—The integration of Automated Shuttles into shared urban spaces presents unique challenges due to the absence of traffic rules and the complex pedestrian interactions. Accurately anticipating pedestrian behavior in such unstructured environments is therefore critical for ensuring both safety and efficiency. This paper presents a Virtual Reality (VR) study that captures how pedestrians interact with automated shuttles across diverse scenarios, including varying approach angles and navigating in continuous traffic. We identify critical behavior patterns present in pedestrians’ decision-making in shared spaces, including hesitation, evasive maneuvers, gaze allocation, and proxemic adjustments. To model pedestrian behavior, we propose GazeX-LSTM, a multimodal eye gaze-informed and context-aware prediction model that integrates pedestrians’ trajectories, fine-grained eye gaze dynamics, and contextual factors. We shift prediction from a vehicle- to a human-centered perspective by leveraging eye-tracking data to capture pedestrian attention. We systematically validate the unique and irreplaceable predictive power of eye gaze over head orientation alone, further enhancing performance by integrating contextual variables. Notably, the combination of eye gaze data and contextual information produces super-additive improvements on pedestrian behavior prediction accuracy, revealing the complementary relationship between visual attention and situational contexts. Together, our findings provide the first evidence that eye gaze-informed modeling fundamentally advances pedestrian behavior prediction and highlight the critical role of situational contexts in shared-space interactions. This paves the way for safer and more adaptive automated vehicle technologies that account for how people perceive and act in complex shared spaces.

Index Terms—Shared spaces; virtual reality; eye tracking; automated shuttles; pedestrian trajectory prediction; multimodal learning; context-aware prediction.

I. INTRODUCTION

THE emergence of automated shuttles offers promising solutions for sustainable and efficient last-mile transportation. Yet, their integration into urban environments raises new challenges, especially in shared spaces where no traffic rules are imposed. As shown in [1], pedestrians exhibit significant behavioral changes when encountering small automation-capable vehicles in such settings. Thus, understanding and predicting pedestrian behavior in these contexts is crucial for ensuring a harmonious coexistence in futuristic scenarios. However, most existing research on pedestrian-autonomous vehicle (AV) interactions has focused on structured environments, particularly crossing scenarios [2]. Only limited studies

have examined the more diverse and complex interactions occurring in shared spaces, and even then, the emphasis is often on perpendicular and road-crossing-like interactions [3]–[5]. Moreover, prior work has largely addressed homogeneous pedestrian-pedestrian interactions or interactions with conventional passenger cars [2]. Interactions involving automated shuttles that have distinct sizes, speeds, and dynamics remain insufficiently studied.

Field experiments with automated shuttles have provided insights into such interactions, but critical situations are rare due to the shuttles’ conservative operations and low speeds in the real world [6]. As such, immersive technologies like Virtual Reality (VR) have become a powerful alternative, enabling safe, controlled, and reproducible study of pedestrian-automated shuttle interactions [3], [7], [8]. Meanwhile, VR allows us to capture brief actions of pedestrians that would be difficult to capture in real-world settings, such as small steps, hesitations, or glances [9]. Except for these benefits, VR-based experiments also provide a unique opportunity to analyze the interactions from a human-centered perspective through the integration of eye-tracking data. This paradigm shift from the vehicle to the pedestrian can offer insights into pedestrians’ perception and intention that trajectories alone cannot. For example, a pedestrian walking fast could either signal danger if frequently checking the vehicle, or confidence if not looking at all. Prior research has also recognized attention as a key correlate of locomotion, destination, and path planning [10]–[12]. In the context of pedestrian trajectory prediction, attention is often approximated by head orientation and has been shown to improve prediction accuracy [13]–[16]. Other studies have leveraged semantic cues like attention and eye contact detected from vehicle-mounted cameras [17]–[19]. Though incorporating eye gaze data holds strong potential, predicting pedestrian behavior directly from a human perspective has not been explored.

To improve trajectory prediction accuracy, many studies have incorporated contextual information beyond motion data. Commonly used contexts include scene information represented by high-definition maps [20], [21], social context showing the influence of surrounding agents [22], [23], and behavioral contexts encoding intentions and goals [24], [25]. These forms of context have shown strong predictive power. However, relatively fewer studies have explored situational context, such as traffic parameters, environmental conditions, or other external factors that describe the broader conditions under which interactions occur [26]–[28]. Moreover, some of the contextual cues leveraged in structured environments

Danya Li and Rico Krueger are with the Department of Technology, Management and Economics at the Technical University of Denmark.

Yan Feng is with the Department of Transport & Planning, Civil Engineering Geosciences at Delft University of Technology.

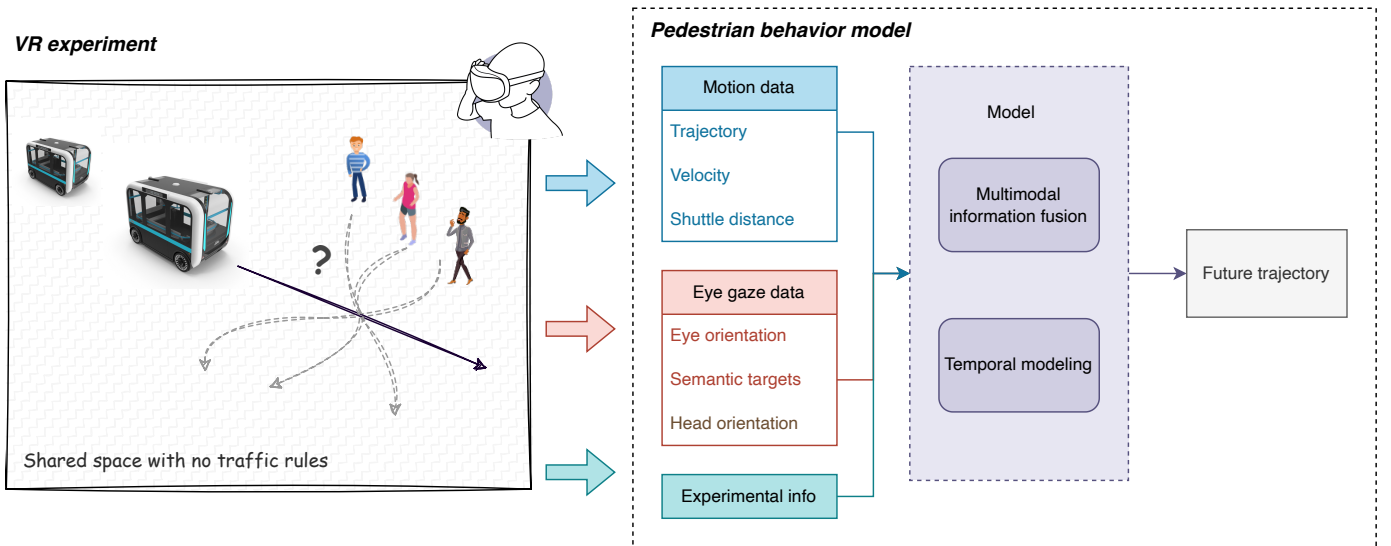


Fig. 1. An overview of the paper.

are absent or less informative in shared spaces. For instance, map-based or infrastructure-related features cannot be directly applied because shared spaces usually lack physical separation. These considerations motivate the need to identify and model alternative situational contexts that meaningfully influence pedestrian behavior in shared spaces.

This paper addresses these gaps through a VR study of pedestrian-automated shuttle interactions in shared spaces. More specifically, we examine scenarios beyond conventional road crossings, including shuttles approaching from multiple angles and/or navigating within continuous traffic, thereby capturing the diversity of shared-space interactions. A dataset of pedestrian motion, fine-grained eye gaze, and situational context is collected for studying micro-level interactions. To predict pedestrian future behavior, we introduce GazeX-LSTM, a multimodal model that fuses motion status, eye gaze, and situational factors and tackles temporal modeling using long-short term memory (LSTM). Fig. 1 provides an overview of our approach.

Our contributions are threefold. Firstly, we present a novel contribution on pedestrians and multiple vehicles interactions in shared spaces, considering previously unexplored factors like approach angles and continuous traffic. By analyzing critical behaviors like hesitation, deviation, gaze, and proxemics preference, we empirically characterize pedestrian responses in shared spaces. Secondly, we highlight the benefits of shifting from a vehicle-centered to a human-centered behavior prediction. We comprehensively evaluate the role of eye gaze, exploring various representations of eye gaze orientation and fixations on semantic targets, and compare the predictive value of direct eye gaze data with head orientation as a proxy. Thirdly, we demonstrate how situational context, such as approach angles and traffic contexts, quantitatively and qualitatively influence pedestrian behavior prediction.

The remainder of the paper is structured as follows: Section II reviews related studies on shared-space interactions, eye-tracking applications, and context-aware trajectory predic-

tion. Section III, IV, and V describe the modeling framework, VR experiment, and implementation details. Section VI and VII present and discuss the results with future research directions. The paper ends with a conclusion.

II. RELATED WORKS

A. Pedestrian-AV interaction in shared spaces

Pedestrian-AV interaction has received a lot of attention in recent years. Numerous publicly available datasets capture the trajectories of pedestrians and vehicles interacting with each other (e.g., INTERACTION [29], Waymo [30], nuScenes [31], JAAD [17], PIE [32]). However, most of these datasets are collected in structured traffic settings such as intersections and crosswalks, primarily focusing on road-crossing scenarios. In contrast, the more complex unstructured shared spaces where no explicit traffic rules are imposed have been studied far less extensively [2]. Only a limited number of real-world datasets capture such interactions (e.g., HBS [33], DUT [4], CTR [4], and USyd [34]), and these remain limited in scale and complexity. Simulator-based studies have also explored such interactions under controlled conditions [3], [7], [8]. Yet, these works generally focus on perpendicular interactions [5]. In practice, shared spaces involve a much broader range of encounter geometries, where pedestrians and AVs may approach each other from the front, the side, or even from behind. Insights from human-robot interaction suggest that pedestrians' responses vary considerably depending on the robot's approach angle [35], [36], but this effect has not been investigated in pedestrian-AV interaction research [37].

Existing studies on shared spaces have concentrated on interactions between pedestrians and conventional passenger vehicles, as well as on homogeneous pedestrian-pedestrian interactions. Automated shuttles, as a natural agent in shared spaces, are often overlooked [7]. A previous study [38] suggested that pedestrians perceive automated shuttles differently from conventional vehicles. A field study in Sydney also showed that pedestrians adapt their behavior significantly

when interacting with small and automation-capable vehicles [34]. Similarly, [6] conducted field experiments with automated shuttles in both road and shared space environments, but their analysis is limited to basic statistical analysis, as critical situations were rare due to the shuttles' conservative settings and low operating speeds. Overall, research on pedestrian-automated shuttle interaction in shared spaces is still insufficient.

Modeling pedestrian-AV interaction in shared spaces can be broadly divided into three categories: expert-based, data-driven, and hybrid models. Expert-based models provide the most explainability, and social force models (SFM) [39] are the most widely used ones. SFMs consider repulsive and attractive forces from collision avoidance, social interactions, etc [40]–[42]. [43] developed a probabilistic model with a risk-based attention mechanism to predict when pedestrians yield, followed by an SFM-inspired component that captures vehicle influence on pedestrian motion during yielding. Data-driven approaches are also used to achieve higher accuracy [44]–[47], among which LSTM-based models are especially common: [44] integrate spatial repulsive forces (resulting from occupancy) and temporal repulsive forces (based on time-to-collision) into an LSTM, whereas [45] combine an LSTM with interactive collision probabilities for pedestrian trajectory prediction. Finally, hybrid approaches seek to balance predictive accuracy with interpretability by combining data-driven models with expert-based components [48], [49]. For instance, [48] propose a framework where an LSTM-DBSCAN deep learning model is complemented by an expert model (SFM and game theory) whenever conflicts arise in predictions.

Our work thus focuses on the natural shared-space interactions between pedestrians and automated shuttles. We account for various approach angles and continuous traffic flow that are present in real-world environments. To model these interactions, we adopt an LSTM-based predictive framework given its established role in pedestrian trajectory prediction.

B. Eye gaze in pedestrian behavior analysis

The interests in applying eye gaze data span multiple domains [50], such as enhancing human-computer interaction [51], evaluating training and learning [52], supporting decision-making in marketing [53], [54], and aiding clinical diagnosis [55]. In traffic contexts, eye movements have been shown to be closely linked to physical activities [10] and to correlate with a person's destination and walking path [11], [12]. In what follows, we review how eye tracking and attention have been incorporated into the pedestrian behavior analysis literature.

In trajectory prediction literature, head orientation is often used as a proxy for human attention as eye-tracking data is unavailable [13]–[16]. It can be extracted from visual input recorded from the vehicle's perspective [14], [15], [56] and has been shown to provide useful predictive cues. For instance, [13] found that head pose correlates strongly with movement at high speeds, although this correlation weakens when pedestrians slow down. Similarly, [14] demonstrated that combining motion with head pose improves trajectory

prediction accuracy. Collectively, these findings highlight the value of head orientation as an attention indicator. However, how eye gaze data can further influence prediction remains unexplored in this context.

Eye-tracking data can be readily collected in controlled experiments using dedicated equipment, and has been applied in several VR-based studies on pedestrian-AV interactions [3], [57]–[63]. It is typically analyzed using the Area-of-Interest (AoI) method, where visual attention is aggregated into predefined regions, ranging from broad traffic-related areas [3], [57] to more specific AV components [58]. Based on these AoIs, eye movement measures are then summarized into higher-level variables like duration, frequency, and distribution. These aggregated gaze features are then used to evaluate AV interface design [58], [59], study distraction effects [57], or approximate mental workload [58], [59].

Another related line of work is to use eye gaze for locomotion prediction in redirected walking [64]–[68]. Here, gaze has been found to provide task- and environment-dependent benefits. For example, [64]–[66] show that situations with walking speed changes benefit from using eye data. [67] argued that gaze can reduce prediction errors in low-distraction scenarios, but increase errors under high-distraction conditions.

Our work then leverages eye-tracking data collected in VR experiments to allow a human-centered behavior prediction. We investigate to what extent precise eye gaze information can enhance predictive modeling and whether it can be effectively substituted with the approximated head orientation commonly used in the literature.

C. Context-aware trajectory prediction

Trajectory prediction has moved toward context-aware approaches that leverage information from multiple sources. Commonly used contexts include scene information represented by high-definition maps [20], [21], social context showing the influence of surrounding agents [22], [23], and behavioral contexts encoding intentions and goals [24] or representing actions [25]. These forms of context have shown strong predictive power.

A relatively smaller number of studies have examined situational context variables that capture external or scenario-level factors shaping the interactions [26]–[28]. For instance, [26] examined the effects of road specifications (lane width, type of road), traffic parameters (speed limit, arrival rate), and environmental conditions (weather conditions, time of the day) while [27] modeled the effects of crossing facilities. A number of studies have also investigated the effects of external human-machine interfaces (eHMIs) on pedestrian-AV interaction [3], [69], [70]. These situational factors have been more commonly investigated in the human factors field, but their quantitative effects for trajectory prediction are still limited.

Our work explores the effects of several situational context factors, including approach geometry, vehicle behavior, eHMI presence, and continuous traffic, on the predictive power of pedestrian models for shared spaces.

III. METHODOLOGY

A. Problem definition

We aim to predict pedestrians' future trajectories based on their past behaviors. Mathematically, our goal is to learn a function \mathcal{F} to map the pedestrian's past trajectories \mathbf{Y}^{past} , additional time series in the past \mathbf{S} , and experimental variables \mathbf{X} to the future trajectories \mathbf{Y}^{fut} , formulated as:

$$\mathbf{Y}^{fut} = \mathcal{F}(\mathbf{Y}^{past}, \mathbf{S}, \mathbf{X}) \quad (1)$$

Pedestrian future trajectories are $\mathbf{Y}^{fut} = \{\mathbf{Y}_{T_p+1}, \mathbf{Y}_{T_p+2}, \dots, \mathbf{Y}_{T_p+T_f}\} \in \mathbb{R}^{N \times T_f \times 2}$, where $\mathbf{Y}_t = [\mathbf{y}_{1t}, \mathbf{y}_{2t}, \dots, \mathbf{y}_{Nt}]^T \in \mathbb{R}^{N \times 2}$, $\mathbf{y}_{nt} \in \mathbb{R}^2$ denotes the trajectory coordinates of data point n at time t , N denotes the number of data points, and T_p and T_f is the length of the past and future time steps, respectively. In our problem, both T_p and T_f are 2 seconds with a 20 Hz frequency, which corresponds to 40 time steps. The prediction is based on the following three groups of data:

- 1) pedestrians' trajectory in the past $\mathbf{Y}^{past} = \{\mathbf{Y}_1, \mathbf{Y}_2, \dots, \mathbf{Y}_{T_p}\} \in \mathbb{R}^{N \times T_p \times 2}$;
- 2) additional time series observations $\mathbf{S} = \{\mathbf{V}, \mathbf{D}, \mathbf{E}\}$, including pedestrians' speed $\mathbf{V} \in \mathbb{R}^{N \times T_p \times N_v}$, pedestrians' distance to shuttles $\mathbf{D} \in \mathbb{R}^{N \times T_p \times N_d}$, and eye gaze or head data $\mathbf{E} \in \mathbb{R}^{N \times T_p \times N_e}$;
- 3) experimental variables $\mathbf{X} \in \mathbb{R}^{N \times 4}$, including eHMI presence, whether the shuttles yield or not, approach angle, and continuous traffic;

B. Model architecture

As reviewed in Sec. II-A, deep learning techniques, particularly the LSTM model [39], are widely used for pedestrian behavior prediction. Building on this foundation, we developed a trajectory prediction model that fuses multimodal information through modality-specific LSTM encoders. The model architecture is illustrated in Fig. 2.

The model integrates both dynamic and static inputs:

- **Motion features:** past pedestrian trajectories and velocities [26], [43].
- **Distance features:** relative distances between pedestrians and automated shuttles, which have been shown to be critical for interaction modeling [26].
- **Eye gaze features:** time series data capturing gaze direction or semantic targets, newly collected in our experiments.
- **Situational variables:** static experimental variables described above.

Each dynamic input stream is encoded with a dedicated LSTM, while situational variables are concatenated directly with the encoded representations. The fused latent representation is then passed to the decoder, consisting of fully connected dense layers with ReLU activations, which outputs predictions for all future time steps in a single forward pass. We adopted the general framework from [26] as the basis for our study. In the mathematical form, the neural network architecture is as follows:

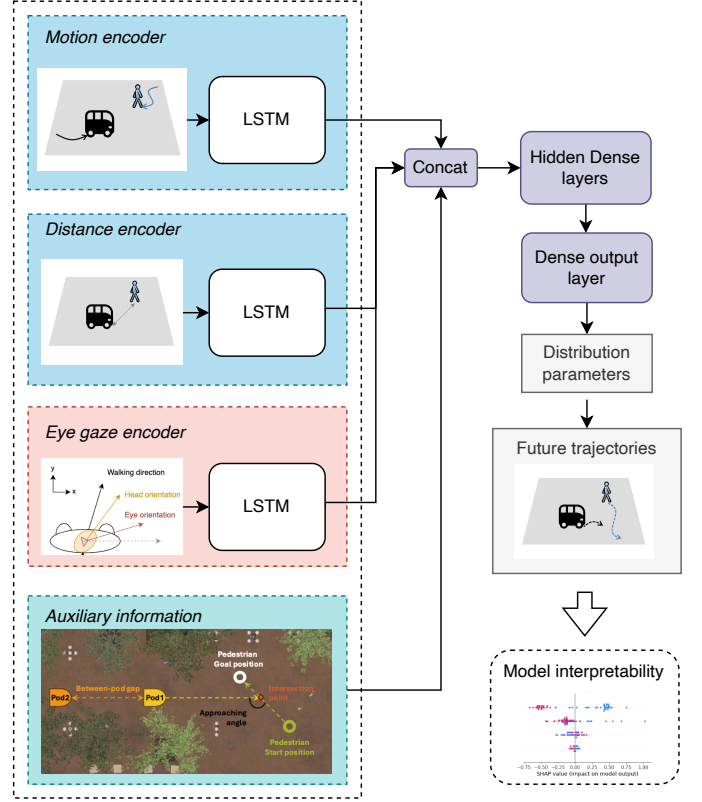


Fig. 2. Model architecture.

- LSTM motion encoder:

$$\mathbf{H}_m = \text{LSTM}(\mathbf{Y}^{past}, \mathbf{V}, \mathbf{W}_m, \phi)$$

- LSTM distance encoder:

$$\mathbf{H}_d = \text{LSTM}(\mathbf{D}, \mathbf{W}_d, \phi)$$

- LSTM eye gaze encoder:

$$\mathbf{H}_e = \text{LSTM}(\mathbf{E}, \mathbf{W}_e, \phi)$$

- Hidden dense layers:

$$\mathbf{H}_h = f_h([\mathbf{H}_m, \mathbf{H}_d, \mathbf{H}_e, \mathbf{X}, \mathbf{W}_h, \phi])$$

- Output layer:

$$[\boldsymbol{\mu}, \boldsymbol{\Sigma}] = f_o([\mathbf{H}_h, \mathbf{W}_o, \phi])$$

where $\mathbf{W}_m, \mathbf{W}_d, \mathbf{W}_e$ are the weights of LSTM layers, \mathbf{W}_h and \mathbf{W}_o are the weights of hidden dense and output layers, ϕ is the activation function with ReLU, and f_h and f_o are hidden dense and output layers, respectively.

We assume the future trajectory follows a multivariate Gaussian distribution, i.e., $\mathbf{y}_{nt} \sim \mathcal{N}(\boldsymbol{\mu}, \boldsymbol{\Sigma})$, where $\boldsymbol{\mu} \in \mathbb{R}^2$ and $\boldsymbol{\Sigma} = \mathbf{U}^T \mathbf{U} \in \mathbb{R}^{2 \times 2}$, where \mathbf{U} denotes an upper triangular matrix. Thus, our model predicts five distribution parameters.

C. Eye data representation

The common representations of eye data include the direction of the eyes [13], [15], [16], [64]–[68] and their semantic targets [17]–[19].

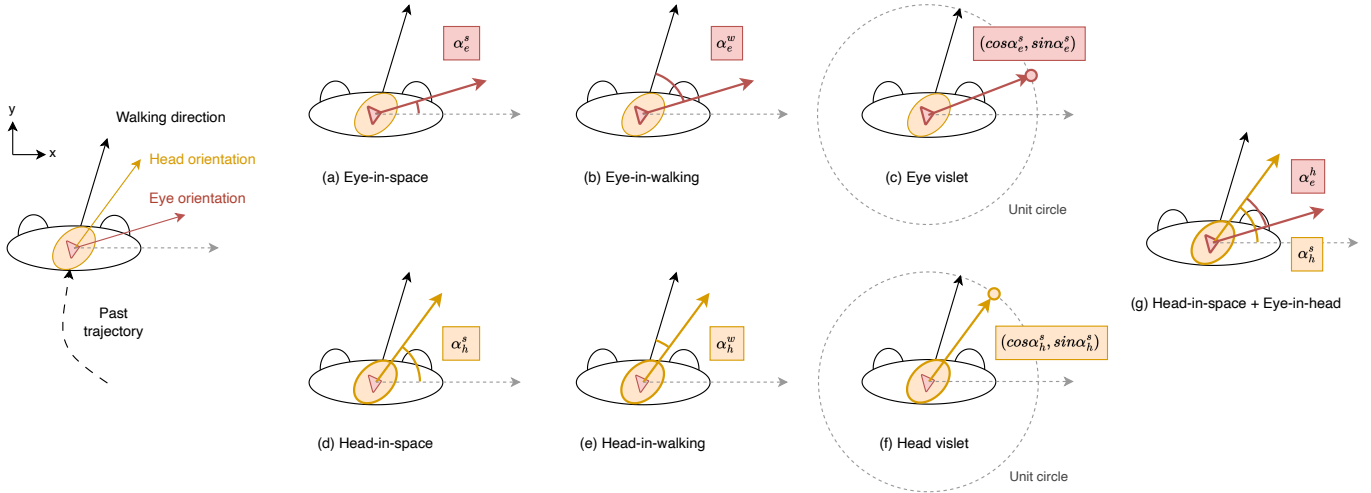


Fig. 3. Representation of eye and head direction in our model. The first row shows the eye representation, and the second row shows the corresponding head representation. The first column uses the world frame as the reference axis, while the second column uses the walking direction as the reference axis. The third column shows the eye/head-in-space representations on a unit circle to avoid the discontinuity brought by angle representation. Subfigure (g) shows the combination of head and eye usage.

We first introduce the eye orientation representation in four formats illustrated in Fig. 3 a-c, g). We are interested in the direction change from the top-down view (indicating the left and right movement of the eyes). They are:

- **Eye-in-space** α_e^s : The absolute degree of eye direction in the world coordinate system, which assumes that the global positioning may contain extra information.
- **Eye-in-walking** α_e^w : The degree of eye direction relative to the pedestrian's walking direction, which assumes that the local positioning is important.
- **Eye vislet** $(\cos \alpha_e^s, \sin \alpha_e^s)$: The reference point at a fixed distance (using the unit circle) from the current location, towards which the eye is oriented [13]. This vislet representation could avoid the discontinuity brought by angle representation and may be more convenient for the vislet-position interplay.
- **Eye+head** (α_h^s, α_e^h) : The absolute head-in-space angle and the associated eye gaze offset (shown in Fig. 3 g)).

To represent and test the effects of semantic target labels, we can formulate different hypotheses about:

- **Gaze events**: Indicators of attention (fixations on any task-related objects like shuttles, goals, and environments), saccades (fixation shifts), and noise (very short fixation sequences).
- **Presence of attention**: Indicator of whether pedestrians' attention is on task-related objects.
- **Attention on traffic**: Indicators of whether pedestrians have attention on shuttles or on others.
- **Attention distribution**: Indicator of which object the pedestrians' attention is on. It can be on the leader shuttle, follower shuttle, goal position, or the environment.

When predicting from a driver's perspective, such eye gaze data is usually unavailable. To further examine the proxy effects of head orientation, we derive the head orientation representation similar to the eye orientation representation as follows, and also show them in Fig. 3 d-f):

- **Head-in-space** α_h^s : The absolute degree of head orientation in the world coordinate system.
- **Head-in-walking** α_h^w : The degree of head orientation relative to the pedestrian's walking direction.
- **Head vislet** $(\cos \alpha_h^s, \sin \alpha_h^s)$: The reference point at a fixed distance (using the unit circle) from the current location, towards which the head is oriented.

IV. VIRTUAL REALITY EXPERIMENT

To test our model, we developed an immersive VR experiment focusing on the specific pedestrian-automated shuttle interactions in shared space. We examined how various factors influence such interactions and collected data for later analysis.

A. Experiment design

1) *Virtual environment*: The virtual environment of a shared space resembling Delft shopping streets was used in VR using Unreal Engine 5 (shown in Fig. 4 b). The environment had no elements that indicated the right of way, i.e., no traffic lights, no stop signs, no pedestrian zebra, and no lane specification for automated shuttles. An audio effect of a noisy shared space and electric automated shuttles was added to enhance the realism of the virtual environment.

2) *Factor design*: Four within-subject variables were included, namely shuttle behavior (i.e., yielding, non-yielding), presence of eHMI (i.e., with eHMI, without eHMI), approach angle (i.e., 45°, 90°, 135°), and continuous traffic (i.e., single shuttle, two shuttles with a gap of 3 seconds, two shuttles with a gap of 5 seconds). An illustration of the last two variables is shown in Fig. 4 a), and a detailed explanation is shown below:

- **Shuttle behavior**: The shuttle can either stop or not stop for pedestrians in a real-world shared space environment. For non-yielding cases, automated shuttles maintained the speed. For yielding cases, we chose the design of type I deceleration profile in [3] and adapted it to detect pedestrians from 12 meters.

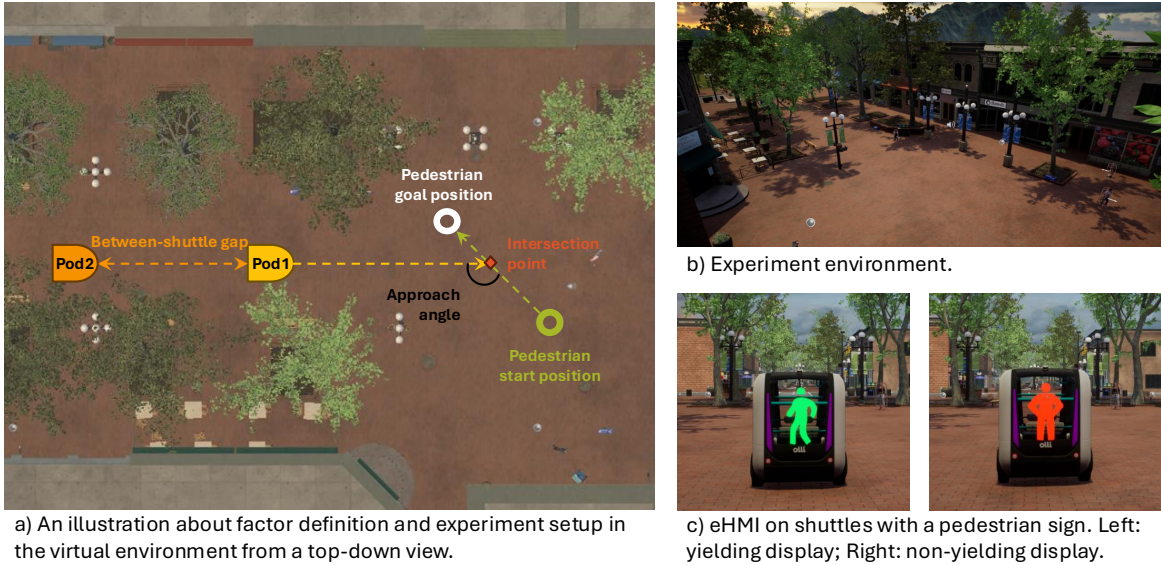


Fig. 4. An overview of the experiment setup.

- *eHMI presence*: The eHMI was designed with a pedestrian sign displayed on the front window when it was activated, shown in Fig. 4 c). Depending on the shuttle's behavior, a red pedestrian signal indicates that the shuttle cannot stop for the pedestrian, while a shuttle signaling green pedestrian signal indicates it will stop in front of the pedestrian.
- *Approach angle*: The angle between the forward directions of the automated shuttles and that of the pedestrian formed the approach angle. The 90° resembled the typical crossing scenario. Additionally, we considered 45° and 135° to examine how visibility influences such interactions.
- *Continuous traffic*: We considered the one-shuttle and two-shuttle interactions. For the two-shuttle interactions, we decided gap size of 3 and 5 seconds, based on literature [38], [71] and our pilot study.

3) *Sampling method*: The combination of all design variables yielded 36 scenarios. However, to reduce participants' fatigue, we determined 12 scenarios per participant based on a pilot study and used the Latin hypercube sampling (LHS) method [72] to sample from all combinations. Unlike random sampling, LHS stratifies the range of each factor into equal intervals and ensures that each interval is sampled exactly once. This approach preserved the Latin square property and thus provided more representative samples.

4) *Experimental task*: At the beginning of each trial, there was a green and a white circle indicating the start and goal positions of the interaction task, respectively. Participants were required to step into the green circle, orient themselves toward the goal, and press the controller when they were ready to walk. Upon walking, the automated shuttle started to approach the pedestrian from a distance of 17.3 meters at a speed of 15 km/h, following the shared space speed limit in the Netherlands. Participants were instructed to reach the goal safely as they would in daily life. The trial ended once

participants reached the goal position, after which the next scenario was initiated.

B. Experiment apparatus

The VR experiment was conducted in a 10×5 meter room. HTC VIVE Pro Eye headset (resolution: 1440×1600 pixels per eye, 110° field of view, 90 Hz refresh rate) was used during the experiment. We also used the real-walking locomotion method, allowing users to have continuous movements and rotations in the real world, which can be matched under a 1:1 scheme to the virtual environment.

Participants' eye movements were recorded using a head-mounted eye-tracking system. The binocular eye-tracker provided the eye-tracking data at a precision of about $0.5\text{--}1.1^\circ$ of visual angle.

C. Experiment procedure

The experiment procedure is summarized in Fig. 5. Upon arrival, participants were provided with written information about the scenario (including the automated shuttle and eHMI design), procedure, and tasks. They then read and signed a consent form to confirm participation. All participants provided informed consent before taking part in our study. Next, participants were equipped with a calibrated VR headset and started a familiarization phase consisting of two stages: 1) to practice moving freely in the virtual environment, and 2) to familiarize the experiment task and the display and behavior of automated shuttles. The formal experiment began after familiarization. Participants were randomly assigned to one of 12 sampled scenarios. After completing each scenario, they returned to the predefined start position for the next trial. After finishing the VR experiment, participants removed the headset and filled in five questionnaires. Each participant received 15 euros as compensation. Ethical approval was granted by the Human Research Ethics Committee of Delft University of Technology (Reference ID 4888).

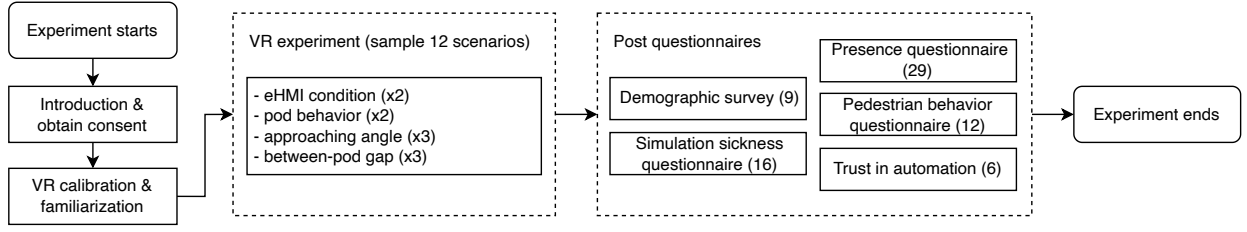


Fig. 5. Experiment procedure. The numbers in the VR experiment block represent the levels of each variable, while the numbers in the post-questionnaire block indicate the number of items in each questionnaire.

D. Data collection

Two types of data were collected during the experiment, including objective and subjective data.

1) *Objective data*: The whole interaction process in the virtual environment was recorded. The data recording started when participants left the start position (at the green circle) and ended when they reached the goal position (at the white circle). The collected data included: 1) timestamp, 2) participant's position, 3) head orientation, 4) eye gaze direction, fixation point, and fixation object. All data were recorded at 20 Hz.

2) *Subjective data*: The subjective part included several questionnaires, namely 1) personal characteristics, 2) simulation sickness questionnaire (SSQ), 3) presence questionnaire (PQ), 4) pedestrian behavior questionnaire (PBQ), and 5) trust in automation. Personal characteristics included age, gender, nationality, highest education level achieved, dominant hand, walking frequency in daily life, familiarity with VR, familiarity with the concept of automated shuttles, and previous experience regarding interaction with automated shuttles. The simulation sickness questionnaire was adopted from [73] to measure the experienced simulation sickness of participants in the virtual environment. The presence questionnaire from [74] measured the feeling of presence in the virtual environment. The pedestrian behavior questionnaire [75] measured three behavior scores that were relevant to people's attention, namely violation, lapse, and positive behaviors. Finally, trust in automation was adopted from [76].

E. Participants

In total, 51 participants aged between 21 and 61 ($M=26.62$, $SD=5.76$) were recruited. All participants had normal vision or corrected vision and normal mobility. None of the participants dropped out of the experiment due to motion sickness. The participant characteristics are shown in Tab. I. Each participant completed 12 trials in total. The total number of trials amounted to 612. Removing those trials that were mistakenly triggered, with missing eye tracking signals, and with lost VR signal, we obtained 537 trials.

F. Data analysis

To characterize pedestrian behavior in shared spaces, we derived the following metrics in five groups:

- Movement behavior:

- *Gap selection*: The gap participants chose to cross (i.e., before the first shuttle, between two shuttles, after the last shuttle).

TABLE I
DEMOGRAPHIC INFORMATION OF PARTICIPANTS.

Description	Category	Number (%)
Gender	Male	27 (52.94%)
	Female	24 (47.06%)
Dominant hand	Right hand	47 (92.16%)
	Left hand	4 (7.84%)
Highest education level	High school or eq.	2 (3.92%)
	Associate degree or eq.	0 (0.00%)
	Bachelor's degree or eq.	19 (37.25%)
	Master's degree or eq.	26 (50.98%)
Previous experience with VR	Doctoral degree or eq.	4 (7.94%)
	Never	17 (33.33%)
	Seldom	23 (45.10%)
	Sometimes	10 (19.61%)
Familiarity with the concept of automated shuttles	Often	1 (1.96%)
	Very often	0 (0.00%)
	Not at all	5 (9.80%)
	Slightly familiar	17 (33.33%)
Previous experience with automated shuttles	Moderate familiar	19 (37.25%)
	Very familiar	7 (13.73%)
	Extremely familiar	3 (5.88%)
	No experience	27 (52.94%)
Previous experience with automated shuttles	Little experience	13 (25.49%)
	Some experience	10 (19.61%)
	A lot of experience	1 (1.96%)
	Extensive experience	0 (0.00%)

- *Waiting time*: The time from the trial started to the participants' last movement initiation.
- Hesitation behavior:
 - *Initiation count*: The total number of crossing attempts made by the pedestrian during a trial, including the final successful crossing. An attempt is formally registered when the pedestrian's velocity exceeds the defined crossing initiation speed (see Sec. V-C1).
 - *Backward count*: The total number of instances in a trial where the pedestrian stepped backward. A backward step is registered when the pedestrian's velocity is below the backward velocity threshold (see Sec. V-C1).
- Deviation behavior:
 - *Mean deviation*: The average lateral offset between the participant's actual path and the ideal straight-line path.
 - *Max. deviation*: The maximal lateral offset between

the participant’s actual path and the ideal straight-line path.

- Gaze behavior:
 - *Pre-crossing shuttle-gaze time*: The time that participants focused on the shuttle before starting their crossing.
 - *During-crossing shuttle-gaze time*: The total time that participants focused on the shuttle while crossing.
- Proxemics:
 - *Lateral clearance*: The lateral distance between the participant and the shuttle as it passed.

V. IMPLEMENTATION DETAILS

A. Metrics

Two metrics are considered to evaluate the performance:

- The average displacement error (ADE) or the mean squared error (MSE): The average Euclidean distance between ground-truth and prediction trajectories over all predicted time steps, as defined below, where the predicted position for n -th pedestrian at time step t is $\hat{\mathbf{y}}_{nt} \in \mathbb{R}^2$ and the ground-truth is \mathbf{y}_{nt} :

$$ADE = \frac{1}{N \times T_f} \sum_{n=1}^N \sum_{t=T_p+1}^{T_f} \|\mathbf{y}_{nt} - \hat{\mathbf{y}}_{nt}\|_2$$

- The final displacement error (FDE): The average distance between ground-truth and prediction trajectories for the final predicted time-step, as defined below:

$$FDE = \frac{1}{N} \sum_{n=1}^N \|\mathbf{y}_{n, T_p+T_f} - \hat{\mathbf{y}}_{n, T_p+T_f}\|_2$$

We consider predictions in two modes:

- Deterministic: Mean prediction (evaluated at μ).
- Stochastic: The best prediction out of 20 random predictions, denoted as min-20 later.

B. Baseline

Our baseline is the LSTM that only uses the input of pedestrians’ trajectory, velocity, and distance between shuttles and pedestrians to predict the pedestrians’ future trajectory, without incorporating experimental scenarios. This allows isolating the contribution of gaze and context when introduced later.

C. Data preparation

1) *Motion data preprocessing*: We smooth both pedestrian trajectories and speed profiles using a Gaussian filter with $\sigma = 4$. Sequences in which shuttles moved before pedestrians are treated as false triggers and removed, along with data containing missing eye-tracking or lost VR signals.

To identify initiation time points, we apply a histogram-based thresholding algorithm to velocity data, following the procedure of [77]. Since multiple initiation points may occur, we define the transition between pre-crossing and crossing stages using the last initiation point before pedestrians step onto the shuttle paths. We conducted the same procedure to determine the backward velocity threshold.

2) *Eye gaze data preprocessing*: To preprocess eye orientation data, we primarily address missing values caused by blinks and saccades. Following the recommendations of [78], we apply linear interpolation to fill missing values and remove data segments 0.1 seconds before and after each gap to minimize artifacts introduced by gaps.

For extracting semantic gaze targets, we post-process fixation data obtained from the built-in eye trackers. These raw fixations classify gaze on the leader shuttle, follower shuttle, goal position, and other elements (e.g., environment, neighboring objects), but they are noisy and require refinement. Firstly, we detect the saccades that involve the high-speed ballistic eye movement using the instantaneous velocity thresholding (I-VT) method [79] with a threshold of 100°/second for angular eye-in-world velocity. For non-saccades gaze points, we smooth the data by replacing the isolated fixation detections with the nearest semantic target. Short gaps that are less than 0.4 seconds [80] and surrounded by identical target values are filled with the surrounding target value, as they are likely caused by blinks; otherwise, sequences shorter than 0.1 seconds are masked as noise. This procedure yields reliable indicators for attention allocation to each object, saccades, and noise.

Moreover, the experimental variables are categorically encoded.

3) *Data summary*: After all the pre-processing steps, we obtain our final data. We split the data into training, validation, and test based on individuals, and the ratio is 6:1:3. For each trial, the split is on a sliding window with a stride of 4 for a trade-off between redundancy and information. This results in a training set of size 11916, a validation set of 1640, and a test set of 3918.

D. Interpretation method

To interpret our black-box model and the effects of experimental variables on the prediction outputs, we use SHAP (SHapley Additive exPlanations), a post-hoc game theory interpretation method [81]. It works by explaining individual predictions by calculating the contribution of each feature using concepts from game theory. Having a positive SHAP value for a variable in an instance means a higher output due to the presence of that factor. We used the GradientExplainer to estimate Shapley values based on the expected gradients. 100 random background samples and then 50 random samples are used for plotting. We choose the last time step that is associated with the goal position, and evaluate on the mean prediction.

VI. RESULTS

A. Descriptive analysis

Tab. II summarizes descriptive statistics for the five groups of indicators described in Sec. IV-F. Shuttle yielding behavior generally facilitates crossing and reduces hesitation behavior, as indicated by shorter waiting times, fewer initiation and backward steps, smaller deviations, and shorter pre-crossing gaze time at shuttles. At the same time, pedestrians tend to spend more time observing shuttles during the crossing and

TABLE II
DESCRIPTIVE STATISTICS FOR MOVEMENT, HESITATION, DEVIATION, GAZE, AND PROXEMICS VARIABLES.

Measures	Shuttle behavior		eHMI presence		Approach angle			Continuous traffic		
	Non-yielding	Yielding	Absent	Present	45°	90°	135°	1 shuttle	2 shuttles (gap=3s)	2 shuttles (gap=5s)
<i>Movement behavior</i>										
<i>Gap selection [count]</i>										
Before the first shuttle	82	261	178	165	117	106	120	101	121	121
Between two shuttles	109	4	54	59	25	51	37	79	2	32
After two shuttles	80	1	37	44	31	26	24	0	55	26
<i>Waiting time [second]</i>										
Mean	6.67	4.32	5.52	5.49	5.48	5.69	5.34	5.02	6.03	5.47
Standard deviation	4.30	3.31	4.06	3.98	3.95	3.92	4.18	3.16	4.42	4.31
<i>Hesitation behavior</i>										
<i>Initiation frequency [count]</i>										
Mean	1.62	1.52	1.57	1.57	1.61	1.54	1.57	1.54	1.56	1.61
Standard deviation	0.65	0.66	0.65	0.67	0.70	0.58	0.70	0.57	0.65	0.75
<i>Backward frequency [count]</i>										
Mean	0.17	0.06	0.10	0.12	0.14	0.07	0.14	0.10	0.10	0.15
Standard deviation	0.42	0.24	0.34	0.35	0.38	0.25	0.39	0.30	0.31	0.41
<i>Deviation behavior</i>										
<i>Mean deviation [cm]</i>										
Mean	22.73	20.65	21.93	21.47	25.08	12.97	27.31	20.46	23.13	21.53
Standard deviation	22.75	20.13	21.85	21.17	25.91	7.66	23.56	17.50	23.72	22.80
<i>Max. deviation [cm]</i>										
Mean	47.83	43.75	46.44	45.18	50.06	28.16	59.59	41.71	49.79	45.44
Standard deviation	44.39	36.94	40.75	41.08	46.12	16.16	46.44	32.37	46.42	42.47
<i>Gaze behavior</i>										
<i>Pre-crossing shuttle-gaze time [second]</i>										
Mean	5.31	3.48	4.44	4.37	4.09	4.60	4.52	4.02	4.93	4.28
Standard deviation	3.68	2.87	3.49	3.37	3.24	3.35	3.66	2.73	3.78	3.63
<i>During-crossing shuttle-gaze time [second]</i>										
Mean	3.31	3.99	3.64	3.65	3.57	3.30	4.07	3.37	3.81	3.76
Standard deviation	1.42	1.99	1.78	1.73	1.86	1.52	1.80	1.39	1.82	1.98
<i>Proxemics behavior</i>										
<i>Lateral clearance [cm]</i>										
Mean	111.80	128.48	111.13	113.20	109.05	125.12	98.87	114.21	108.52	113.17
Standard deviation	44.94	78.30	47.38	44.66	34.30	55.36	37.36	47.60	40.70	48.67

maintain larger lateral clearance beforehand. Interestingly, the presence of eHMI appears to only slightly increase hesitation via more backward steps and has little overall impact on deviation or gaze behaviors.

The approach angle strongly influences interaction patterns. Non-standard angles (45° and 135°) increase hesitation, showing greater uncertainty compared to standard 90° crossings. They also lead to greater deviation, as pedestrians tend to adjust their paths to align more closely with a 90° interaction. In addition, non-standard angles extend gaze duration during crossing, reduce gaze time before crossing, and decrease lateral clearance. Among them, obtuse angles at 135° in particular, produce the most hesitation, largest deviation, and smallest lateral distance, together with increased attention to traffic before crossing and reduced attention to traffic during crossing. This effect is likely due to better visibility in obtuse-angle conditions compared to the standard crossings. Finally, scenarios with two shuttles with 5-second gaps produce higher hesitation and smaller lateral clearance, highlighting the added

complexity in decision-making under such conditions.

In summary, these findings show several variations in hesitation, spatial negotiation, and trajectory deviations across different interaction conditions, revealing pedestrians' critical responses to ambiguous situations. This provides empirical evidence to understand pedestrian behavior and to inform more effective predictive models of shared-space interactions.

B. Results from predictive modeling

1) *Effects of eye gaze information:* Tab. III reports the results of incorporating different forms of eye gaze information into the model. To isolate the effect, contextual information is excluded, and only the eye gaze information is added relative to the baseline.

The type of eye data used, i.e., whether using eye orientation or semantic gaze labels, has a substantial impact on performance. Overall, the incorporation of eye orientation improves behavioral prediction significantly, although the effectiveness depends on how it is represented. Continuous representation

TABLE III

MODEL PERFORMANCE COMPARISON. HORIZON REPRESENTS THE NUMBER OF PREDICTED TIME STEPS, AND ONE TIME STEP CORRESPONDS TO 0.05 SECONDS. THE NUMBERS ARE IN CENTIMETERS. THE BEST RESULTS ARE SHOWN IN **BOLD**, WHICH INDICATES THE LOWEST PREDICTION ERROR. THE BEST RESULTS WHEN INCLUDING SEMANTIC TARGETS ARE SHOWN AS UNDERLINED.

Horizon	Baseline	Eye orientation					Semantic targets			
		eye-in-space	eye-in-walking	eye vislet	eye+head	gaze events	attention presence	attention on traffic	attention distribution	
5	0.05	0.06	0.05	0.08	0.06	<u>0.06</u>	<u>0.06</u>	<u>0.07</u>	0.09	
10	0.27	0.30	0.27	0.29	0.30	<u>0.28</u>	<u>0.28</u>	<u>0.28</u>	0.32	
15	1.11	1.17	1.11	1.08	1.12	1.12	1.12	<u>1.10</u>	1.16	
20	3.51	3.63	3.48	3.38	3.50	3.55	3.55	<u>3.53</u>	3.54	
25	7.51	7.63	7.38	7.21	7.49	7.54	7.54	<u>7.54</u>	<u>7.44</u>	
30	12.47	12.63	12.18	11.95	12.49	12.52	12.52	12.52	<u>12.23</u>	
35	17.94	18.25	17.49	17.22	18.00	18.06	18.06	18.08	<u>17.53</u>	
40/FDE	23.90	24.43	23.28	22.95	23.91	24.13	24.13	24.12	<u>23.29</u>	
ADE	7.09	7.23	6.93	6.81	7.10	7.14	7.14	7.14	<u>6.98</u>	

(a) Mean prediction

Horizon	Baseline	Eye orientation					Semantic targets			
		eye-in-space	eye-in-walking	eye vislet	eye+head	gaze events	attention presence	attention on traffic	attention distribution	
5	0.06	0.09	0.07	0.10	0.08	<u>0.08</u>	<u>0.08</u>	0.09	0.12	
10	0.32	0.37	0.32	0.36	0.36	<u>0.34</u>	<u>0.34</u>	0.35	0.40	
15	0.93	0.99	0.93	0.94	0.96	<u>0.93</u>	<u>0.93</u>	0.94	0.99	
20	2.24	2.30	2.22	2.19	2.24	2.26	2.26	<u>2.24</u>	2.26	
25	3.86	3.89	3.82	3.74	3.83	3.92	3.92	<u>3.86</u>	<u>3.80</u>	
30	5.35	5.40	5.30	5.15	5.35	5.44	5.44	5.38	<u>5.22</u>	
35	7.40	7.53	7.31	7.12	7.42	7.55	7.55	7.46	<u>7.21</u>	
40/FDE	11.17	11.35	10.94	10.74	11.04	11.34	11.34	11.19	<u>10.94</u>	
ADE	3.31	3.38	3.27	3.21	3.31	3.37	3.37	3.34	<u>3.28</u>	

(b) Min-20 performance

via eye vislet yields the best performance, followed by relative eye angle with respect to walking direction. By contrast, absolute eye angle in the world frame not only fails to help but can even reduce performance.

Semantic representations, on the other hand, contribute little and may introduce noise to the predictive models. Semantic targets based on gaze events, presence of attention, or attention to traffic do not improve prediction. The only informative feature in this category is the detailed distribution of attention.

2) *Substitution effects of eye gaze direction with head orientation*: Tab. IV compares model performance when eye orientation is replaced by head orientation. To isolate such effects, the contextual information is excluded as well. The results show that head orientation provides limited to no additional predictive value beyond motion and distance, regardless of the encoding representation methods. Moreover, inappropriate representations can even degrade performance.

3) *Effects of experimental information*: Tab. V presents the model performance with or without experimental information across multiple conditions. The results indicate that, regardless of the inclusion and representations of the eye-tracking data, adding experimental information generally improves long-term prediction but can reduce short-term performance. This effect is also supercomposable in some cases when both eye tracking and experimental information are included.

We conducted a SHAP analysis on the best-performing model, GazeX-LSTM, which uses eye orientation represented by eye-in-walking and experimental information, to evaluate the contribution of different experimental variables to pre-

TABLE IV

ABLATION STUDY ON SUBSTITUTING EYE GAZE DIRECTION WITH HEAD ORIENTATION. HORIZON REPRESENTS THE NUMBER OF PREDICTED TIME STEPS, AND ONE TIME STEP CORRESPONDS TO 0.05 SECONDS. THE NUMBERS ARE IN CENTIMETERS. THE BEST RESULTS ARE SHOWN IN **BOLD**. THE BEST RESULTS WHEN USING HEAD ORIENTATION ARE SHOWN AS UNDERLINED.

Horizon	Baseline	Eye orientation			Head orientation		
		eye-in-space	eye-in-walking	eye vislet	head-in-space	head-in-walking	head vislet
5	0.05	0.06	0.05	0.08	0.07	0.07	<u>0.06</u>
10	0.27	0.30	0.27	0.29	0.31	0.29	<u>0.28</u>
15	1.11	1.17	1.11	1.08	1.11	<u>1.10</u>	1.12
20	3.51	3.63	3.48	3.38	<u>3.45</u>	3.50	3.50
25	7.51	7.63	7.38	7.21	<u>7.40</u>	7.47	7.47
30	12.47	12.63	12.18	11.95	<u>12.34</u>	12.44	12.44
35	17.94	18.25	17.49	17.22	<u>17.81</u>	18.00	17.99
40/FDE	23.90	24.43	23.28	22.95	<u>23.78</u>	24.11	24.07
ADE	7.09	7.23	6.93	6.81	<u>7.03</u>	7.10	7.10

(a) Mean prediction

Horizon	Baseline	Eye orientation			Head orientation		
		eye-in-space	eye-in-walking	eye vislet	head-in-space	head-in-walking	head vislet
5	0.06	0.09	0.07	0.10	0.09	0.09	<u>0.08</u>
10	0.32	0.37	0.32	0.36	0.36	0.36	<u>0.35</u>
15	0.93	0.99	0.93	0.94	0.95	<u>0.94</u>	0.95
20	2.24	2.30	2.22	2.19	2.22	<u>2.21</u>	2.22
25	3.86	3.89	3.82	3.74	<u>3.78</u>	3.81	3.82
30	5.35	5.40	5.30	5.15	<u>5.31</u>	5.34	5.34
35	7.40	7.53	7.31	7.12	<u>7.39</u>	7.50	7.42
40/FDE	11.17	11.35	10.94	10.74	<u>11.10</u>	11.30	11.12
ADE	3.31	3.38	3.27	3.21	<u>3.30</u>	3.34	3.31

(b) Min-20 performance

dictive performance. Fig. 6 summarizes the SHAP values separately for the x- and y-axes in the model. A positive SHAP value on the x-axis reflects movement in the shuttle’s direction (referred to as horizontal movement later), while a positive SHAP value on the y-axis reflects backward movement (lateral movement).

Across both axes, the approach angle emerges as a strong predictor. As expected, non-standard approach angles lead pedestrians to maintain the general crossing trajectory implied by the angle, but an interesting result is that pedestrians’ avoidance strategies varied by angles: At 135°, pedestrians exhibit more assertive behavior compared to the average behavior, in which they tend to move toward the shuttle. At 90°, they show a slight horizontal tendency to walk away from the shuttle; At 45°, pedestrians prefer to distance laterally from the shuttle. Notably, the 45° condition exerts a stronger influence than 135°, as reflected by larger and more dispersed SHAP values.

The number of shuttles has both horizontal and lateral influence on prediction outputs. With a single shuttle, pedestrians move away horizontally but approach laterally. In contrast, with two shuttles, pedestrians consistently move backward, regardless of the between-shuttle gap. A wider gap, however, also induces a tendency to move closer laterally.

The shuttle’s yielding behavior has a pronounced lateral effect: pedestrians move closer to the shuttle laterally when the shuttle yields, which aligns with expectations. The presence of eHMI influences both axes, causing pedestrians to move

TABLE V

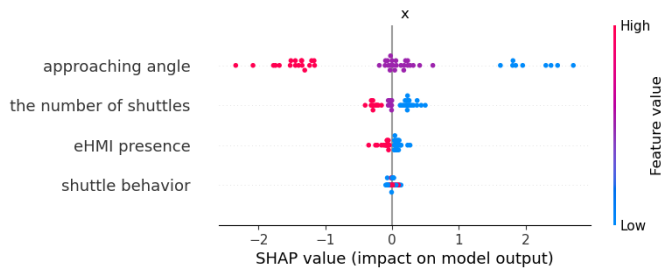
ABLATION STUDY ON THE EFFECTS OF EXPERIMENTAL VARIABLES ON THE PEDESTRIAN BEHAVIOR MODEL. ‘W/O’ STANDS FOR WITHOUT CONSIDERING EXPERIMENTAL INFORMATION, WHILE ‘W/’ STANDS FOR THE INCLUSION. FOR EACH CONDITION, BETTER RESULTS ARE SHOWN IN **BOLD**.

Horizon	Baseline		Eye-in-space		Eye-in-walking		Eye vislet	
	w/o	w/	w/o	w/	w/o	w/	w/o	w/
5	0.05	0.08	0.06	0.07	0.05	0.08	0.08	0.10
10	0.27	0.30	0.30	0.30	0.27	0.31	0.29	0.35
15	1.11	1.15	1.17	1.12	1.11	1.12	1.08	1.18
20	3.51	3.56	3.63	3.48	3.48	3.40	3.38	3.57
25	7.51	7.48	7.63	7.31	7.38	7.12	7.21	7.40
30	12.47	12.22	12.63	11.91	12.18	11.66	11.95	12.02
35	17.94	17.29	18.25	16.89	17.49	16.59	17.22	17.01
40/FDE	23.90	22.66	24.43	22.17	23.28	21.88	22.95	22.32
ADE	7.09	6.90	7.23	6.74	6.93	6.62	6.81	6.82

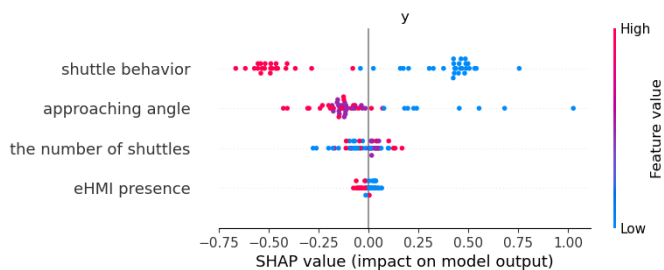
(a) Mean prediction

Horizon	Baseline		Eye-in-space		Eye-in-walking		Eye vislet	
	w/o	w/	w/o	w/	w/o	w/	w/o	w/
5	0.06	0.10	0.09	0.09	0.07	0.10	0.10	0.13
10	0.32	0.38	0.37	0.36	0.32	0.38	0.36	0.43
15	0.93	1.00	0.99	0.96	0.93	0.97	0.94	1.03
20	2.24	2.26	2.30	2.25	2.22	2.19	2.19	2.30
25	3.86	3.79	3.89	3.79	3.82	3.66	3.74	3.84
30	5.35	5.16	5.40	5.11	5.30	4.92	5.15	5.17
35	7.40	7.01	7.53	6.91	7.31	6.62	7.12	6.96
40/FDE	11.17	10.34	11.35	10.21	10.94	9.94	10.74	10.26
ADE	3.31	3.20	3.38	3.16	3.27	3.06	3.21	3.21

(b) Min-20 performance



(a) SHAP analysis on x axis



(b) SHAP analysis on y axis

Fig. 6. Plot summary of the effects of experimental variables on errors.

toward the shuttle, potentially reflecting increased perceived safety.

Taken together, these results highlight that approach angle, number of shuttles, yielding behavior, and eHMI presence meaningfully influence pedestrian responses. We therefore recommend incorporating all these variables when collecting data and modeling pedestrian–automated shuttle interactions.

TABLE VI

SUBSCALES OF SSQ: MEANS AND STANDARD DEVIATIONS

Subscale	Nausea	Oculomotor	Disorientation
Mean	14.74	17.09	35.48
Standard deviation	26.13	22.76	35.55

TABLE VII

SUBSCALES OF PQ: MEANS AND STANDARD DEVIATIONS

Subscale	Involvement	Sensory fidelity	Immersion	Interface quality ¹
Mean	5.71	5.13	5.92	2.25
Standard deviation	0.70	1.00	0.70	1.01

¹ Reversed items.

4) *Qualitative analysis*: We further provide a qualitative analysis of our model in Fig. 7. The first-row plots illustrate the performance improvements by incorporating eye gaze and contextual information. Specifically, the model can predict hesitation behavior (Fig. 7d), recover pedestrians’ normal motion from hesitation (Fig. 7a,c), and maintain lateral distance (Fig. 7b). But there are also cases where our model fails compared to the baseline model, as shown in Fig. 7 (e-g).

C. Results of subjective measures

1) *Simulation sickness*: To measure the extent of simulation sickness participants experienced in the virtual environment, we employed the well-established simulator sickness questionnaire [73]. Using a 4-point Likert scale ranging from 0 (none) to 3 (severe), participants assessed 16 possible symptoms (e.g., eyestrain, nausea, vertigo). The ratings were categorized into three subscales representing symptoms of nausea, oculomotor disturbance, and disorientation. To obtain the subscale scores, the reported scores for each symptom were multiplied by their respective weights for that particular subscale.

The result of each subscale is presented in Tab. VI, in which nausea receives the lowest score and disorientation receives the highest score. The relatively high score of disorientation could be attributed to participants needing to turn and return to their original position after completing each experimental scenario. The average score of the total SSQ is 164.54 (SD = 175.30), and no participants report any discomfort or notable symptoms. According to both SSQ results and participant feedback, the current study reveals no or slight symptoms.

2) *Feeling of presence*: Assessing the feeling of presence is crucial to ensure participants experience an engaging and immersive experience during the VR experiment. We employed the presence questionnaire [74] to measure participants’ sense of presence, which consisted of four subscales, including involvement, sensor fidelity, immersion, and interface quality. Participants rated 29 items using a 7-point Likert scale.

Results of the PQ questionnaire are presented in Tab. VII. The highest score on the immersion subscale indicates that the participants experienced a strong sense of immersion. The average total score of PQ in this study is 151.14 (SD = 17.57), indicating a strong sense of presence in the current study.

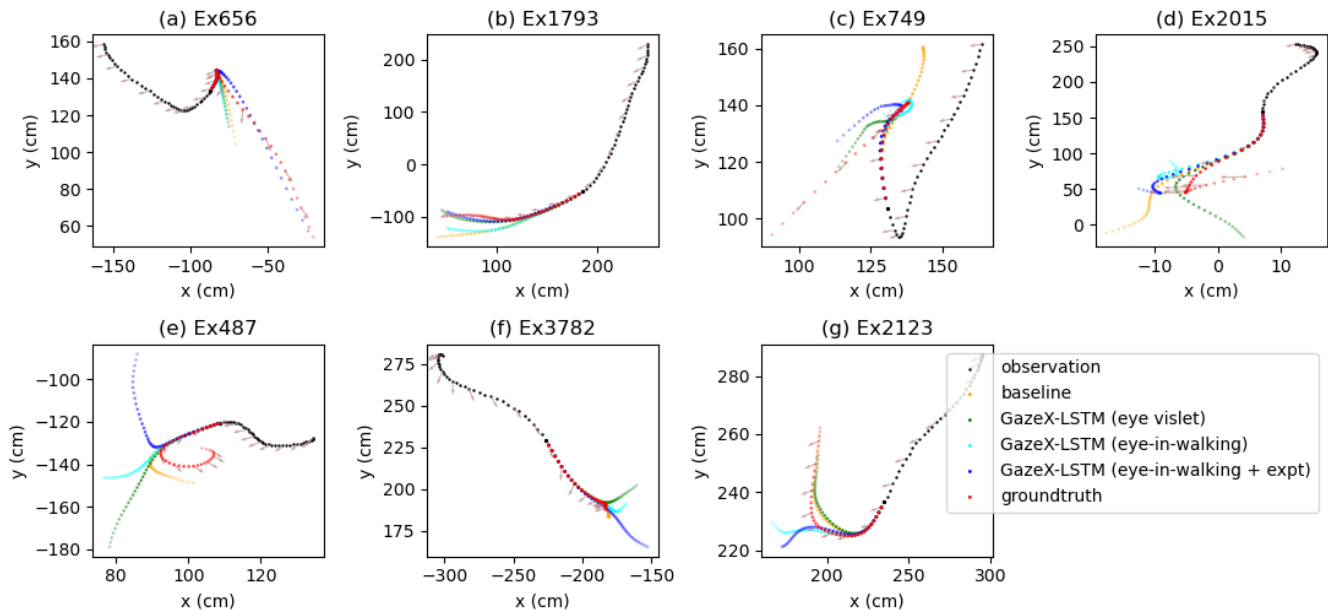


Fig. 7. Qualitative results comparison. The arrows show pedestrians’ eye orientation from the top-down view.

3) *Trust in automation*: The level of trust in AVs was measured per participant using a scale ranging from 1 to 7 [76]. This scale contained questions such as ‘Globally, I trust the automated vehicle’, ‘I trust the automated vehicle to have seen me’, and ‘I trust the automated vehicle to drive safely’. In our experiment, the mean score is 5.18 (SD = 0.86), indicating a moderate level of trust in the AV.

4) *Pedestrian behavior questionnaire*: We evaluated participants’ daily traffic behavior using the pedestrian behavior questionnaire [75]. It measured attention-related tendencies across three categories: violations, lapses, and positive behaviors. Internal consistency is assessed for each category using Cronbach’s alpha. The violation ($\alpha_v = 0.83$) and lapse ($\alpha_l = 0.86$) scales show good reliability. In contrast, the positive behavior scales yield lower consistency ($\alpha_p = 0.60$). After removing item P1 that reduces results’ reliability, the consistency improves to an acceptable level ($\alpha_p = 0.73$). Based on the items with acceptable consistency, the mean score for aggressive behavior is 2.60 (SD = 1.22), for lapse behavior 1.92 (SD = 0.93), and for positive behavior 4.22 (SD = 1.02).

VII. DISCUSSION

A. Interactions in shared spaces

Our analysis highlights several key characteristics of interactions in shared spaces, underscoring the need for greater research attention to this complex environment. These shared spaces can involve subtle behavior adjustments, such as hesitation with more initiation attempts and backward movements, deviation from the shortest paths, and adaptation to proxemics.

In this study, we employed a model without imposing any physical or visual constraints. This allowed us to capture nuanced behavioral patterns such as hesitation, recovery from

hesitation to normal walking, and adaptive lateral distancing in response to the shuttle’s movements.

B. Effects of eye gaze information

We observed that using eye orientation provides substantially greater value for pedestrian trajectory prediction than semantic targets derived from eye gaze. This suggests that fine-grained and continuous information about gaze direction is more informative for operational-level behavior prediction. Coarser event-based information might be more relevant for higher-level tactical or strategic inferences, such as intention or action recognition, as [17] suggested that attentional cues can support action prediction.

Interestingly, we found that including eye gaze data improves long-term prediction performance but can sometimes degrade short-term accuracy. This indicates that recent motion history could be sufficient for short-term predictions, whereas gaze cues carry more information about destination planning and long-term goals. This is consistent with existing work of [11], [12]. These findings highlight the potential of integrating gaze into goal-based prediction frameworks, where it could provide early signals about pedestrians’ intended paths.

Another important observation is that head orientation cannot fully substitute for eye orientation, although it has been frequently used in real-world datasets where eye tracking is unavailable. Prior studies have shown that people rotate their heads more in VR than in natural environments due to the restricted field of view [82], which may reduce the eye-head difference in our dataset. Even though we found that head orientation alone did not enhance prediction, contradicting earlier studies [13]–[16]. One explanation is that head orientation primarily reflects broader attentional shifts, while subtle eye movements capture finer-grained adjustments directly linked to locomotion planning. Differences in measurement fidelity,

environmental context, or the locomotion method may also account for this discrepancy.

C. Effects of experimental variables

Consistent with prior studies [26]–[28], our results demonstrate that incorporating contextual information is highly relevant for pedestrian behavior prediction. Approach angles, the continuous traffic, yielding behavior, and eHMI presence all exert meaningful influences on pedestrian responses, underscoring the importance of incorporating these variables in both future data collection and modeling. In particular, varying approach angles is important to capture the diversity of interaction dynamics in shared spaces.

In our experiments, eHMI presence was found to be the least influential factor affecting pedestrian behavior. However, the effect of eHMI on pedestrian behavior has not yet reached a clear consensus in the literature. While some studies report a positive influence of eHMI on pedestrians’ crossing decisions [83], [84], others suggest that eHMI is not the primary determinant of crossing behavior [69]. This discrepancy may stem from the specific eHMI design, which might not have been sufficiently salient, or from learning effects influencing participants’ perception and belief of the interface. Although we included familiarization trials to mitigate such effects, the adaptation over the course of the experiment cannot be ruled out.

Finally, another notable observation is that contextual information and eye gaze data appear to provide complementary contributions. Their combination shows super-additive effects in some cases. This suggests that context and gaze reflect different layers of decision-making: contextual cues capture external constraints and opportunities in the environment, while gaze signals reveal the pedestrian’s internal allocation of attention and emerging intentions. Together, they provide a richer and more holistic representation of pedestrian behavior than either source alone.

D. Limitations and future work

Despite the findings, several limitations remain that warrant further investigation.

Firstly, our analysis focused primarily on features related to eye movement. Other signals available from eye trackers, such as pupil dynamics or eye status, as well as physiological data from wearable devices like heart rate, could potentially provide more information. Integrating such multimodal signals may further improve predictive power. At the same time, gaze can introduce noise in highly cluttered environments [67]. Future work should also test the robustness of including such information in various environments.

Secondly, our data collection relies on convenience samples of university students. Consequently, the data are highly homogeneous, preventing us from examining the effects of personal characteristics. To better capture individual variability, future research should diversify participant samples across a wider range of demographics, cultural backgrounds, and mobility habits. This would yield more representative data and enable a deeper, more granular analysis of behavioral differences.

Thirdly, our experimental environment was limited to the interaction between a single pedestrian and up to two shuttles. While this allowed us to isolate key mechanisms, it does not capture the full complexity of real-world interactions in shared spaces. Extending experiments to multi-agent scenarios with group behavior and social interactions remains an important direction.

VIII. CONCLUSION

This study explored the intricate dynamics of pedestrian-automated shuttle interactions in shared spaces through a controlled VR experiment. By simulating diverse interaction scenarios with varied approach angles and continuous traffic, we uncovered critical behaviors such as hesitation, deviation, gazing, and proxemics, which are often overlooked yet essential for ensuring safety and efficiency in shared environments. Employing a multimodal LSTM model, we found that fine-grained gaze orientation substantially enhanced trajectory prediction, while coarse semantic targets derived from eye gaze offered limited benefits. Importantly, the benefits brought by eye orientation cannot be fully substituted by head orientation. We also demonstrated that contextual factors, i.e., approach angle, continuous traffic, yielding behavior, and eHMI presence, significantly influence pedestrian behavior. Importantly, eye gaze and situational context contribute complementary signals: their combination yields stronger predictive models than either source alone.

Together, these insights advance our understanding of human-automated shuttle interactions in shared spaces and highlight the value of integrating both human-perspective signals and contextual information in predictive modeling. This becomes especially relevant for future safety applications, as emerging augmented reality (AR) technologies make real-time motion and gaze capture increasingly feasible, supporting proactive risk detection and timely warnings. By capturing the subtle interplay of attention, environment, and behavior, this work helps develop more adaptive and human-aware automated shuttles.

REFERENCES

- [1] Y. Wang, L. Hespanhol, S. Worrall, and M. Tomitsch, “Pedestrian-vehicle interaction in shared space: Insights for autonomous vehicles,” in *Proceedings of the 14th International Conference on Automotive User Interfaces and Interactive Vehicular Applications*, 2022, pp. 330–339.
- [2] M. Golchoubian, M. Ghafurian, K. Dautenhahn, and N. L. Azad, “Pedestrian trajectory prediction in pedestrian-vehicle mixed environments: A systematic review,” *IEEE Transactions on Intelligent Transportation Systems*, 2023.
- [3] Y. Feng, Z. Xu, H. Farah, and B. van Arem, “Does another pedestrian matter? a virtual reality study on the interaction between multiple pedestrians and autonomous vehicles in shared space,” *IEEE Transactions on Intelligent Transportation Systems*, vol. 26, no. 1, pp. 196–209, 2025.
- [4] D. Yang, L. Li, K. Redmill, and Ü. Özgüner, “Top-view trajectories: A pedestrian dataset of vehicle-crowd interaction from controlled experiments and crowded campus,” in *2019 IEEE Intelligent Vehicles Symposium (IV)*. IEEE, 2019, pp. 899–904.
- [5] D. Li, W. Mao, F. C. Pereira, Y. Xiao, X. Su, and R. Krueger, “Analyzing the behaviors of pedestrians and cyclists in interactions with autonomous systems using controlled experiments: A literature review,” *Transportation Research Part F: Traffic Psychology and Behaviour*, vol. 114, pp. 270–307, 2025.

- [6] T. De Ceunynck, B. Pelssers, T. Bjørnskau, O. Aasvik, A. Fyhri, A. Laurshyn, C. Johnsson, M. Hagenzieker, and H. Martensen, "Interact or counteract? Behavioural observation of interactions between vulnerable road users and autonomous shuttles in Oslo, Norway," *Traffic Safety Research*, vol. 2, August 2022.
- [7] R. Woodman, K. Lu, M. D. Higgins, S. Brewerton, P. A. Jennings, and S. Birrell, "Gap acceptance study of pedestrians crossing between platooning autonomous vehicles in a virtual environment," *Transportation Research Part F: Traffic Psychology and Behaviour*, Nov. 2019.
- [8] A. Andrijanto, Z. Chen, T. Kodama, H. Yano, and M. Itoh, "Application of LargeSpace for investigating pedestrians' behaviors when interacting with autonomous vehicles in shared spaces," in *Proceedings - 2022 IEEE Conference on Virtual Reality and 3D User Interfaces Abstracts and Workshops, VRW 2022*, 2022.
- [9] Y. Feng, D. Duives, W. Daamen, and S. Hoogendoorn, "Data collection methods for studying pedestrian behaviour: A systematic review," *Building and Environment*, vol. 187, p. 107329, 2021.
- [10] M. Land and B. Tatler, *Looking and acting: vision and eye movements in natural behaviour*. Oxford University Press, 2009.
- [11] A. E. Patla and J. N. Vickers, "How far ahead do we look when required to step on specific locations in the travel path during locomotion?" *Experimental brain research*, vol. 148, no. 1, pp. 133–138, 2003.
- [12] T. Foulsham, E. Walker, and A. Kingstone, "The where, what and when of gaze allocation in the lab and the natural environment," *Vision research*, vol. 51, no. 17, pp. 1920–1931, 2011.
- [13] I. Hasan, F. Setti, T. Tsesmelis, A. Del Bue, F. Galasso, and M. Cristani, "MX-LSTM: Mixing tracklets and vislets to jointly forecast trajectories and head poses," in *2018 IEEE/CVF Conference on Computer Vision and Pattern Recognition*. Salt Lake City, UT: IEEE, Jun. 2018, pp. 6067–6076.
- [14] D. A. Ridel, N. Deo, D. Wolf, and M. Trivedi, "Understanding pedestrian-vehicle interactions with vehicle mounted vision: An LSTM model and empirical analysis," in *2019 IEEE Intelligent Vehicles Symposium (IV)*, Jun. 2019, pp. 913–918.
- [15] M. Herman, J. Wagner, V. Prabhakaran, N. Möser, H. Ziesche, W. Ahmed, L. Bürkle, E. Kloppenburg, and C. Gläser, "Pedestrian behavior prediction for automated driving: Requirements, metrics, and relevant features," *IEEE Transactions on Intelligent Transportation Systems*, vol. 23, no. 9, pp. 14922–14937, Sep. 2022.
- [16] X. Mo, Z. Huang, Y. Xing, and C. Lv, "Multi-agent trajectory prediction with heterogeneous edge-enhanced graph attention network," *IEEE Transactions on Intelligent Transportation Systems*, vol. 23, no. 7, pp. 9554–9567, 2022.
- [17] A. Rasouli, I. Kotseruba, and J. K. Tsotsos, "Are they going to cross? A benchmark dataset and baseline for pedestrian crosswalk behavior," in *Proceedings of the IEEE international conference on computer vision workshops*, 2017, pp. 206–213.
- [18] Y. Belkada, L. Bertoni, R. Caristan, T. Mordan, and A. Alahi, "Do pedestrians pay attention? Eye contact detection in the wild," Dec. 2021, arXiv:2112.04212 [cs].
- [19] H. Murakami, J. Chen, D. Deguchi, T. Hirayama, Y. Kawanishi, and H. Murase, "Pedestrian's gaze object detection in traffic scene," in *Proceedings of the 19th International Joint Conference on Computer Vision, Imaging and Computer Graphics Theory and Applications*. Rome, Italy: SCITEPRESS - Science and Technology Publications, 2024, pp. 333–340.
- [20] Y. Hu, S. Chen, Y. Zhang, and X. Gu, "Collaborative motion prediction via neural motion message passing," in *Proceedings of the IEEE/CVF conference on computer vision and pattern recognition*, 2020, pp. 6319–6328.
- [21] P. Kothari, D. Li, Y. Liu, and A. Alahi, "Motion style transfer: Modular low-rank adaptation for deep motion forecasting," in *Conference on Robot Learning*. PMLR, 2023, pp. 774–784.
- [22] W. Xiang, Y. Haoteng, H. Wang, and X. Jin, "Socialvae: Predicting pedestrian trajectory via interaction conditioned latents," in *Proceedings of the AAAI Conference on Artificial Intelligence*, vol. 38, no. 6, 2024, pp. 6216–6224.
- [23] C. Xu, M. Li, Z. Ni, Y. Zhang, and S. Chen, "GroupNet: Multiscale hypergraph neural networks for trajectory prediction with relational reasoning," Apr. 2022, arXiv:2204.08770 [cs].
- [24] K. Mangalam, Y. An, H. Girase, and J. Malik, "From goals, waypoints & paths to long term human trajectory forecasting," in *Proceedings of the IEEE/CVF international conference on computer vision*, 2021, pp. 15 233–15 242.
- [25] F. Munir and T. P. Kucner, "Context-aware multi-task learning for pedestrian intent and trajectory prediction," *Transportation Research Part C: Emerging Technologies*, vol. 178, p. 105203, 2025.
- [26] A. Kalatian and B. Farooq, "A context-aware pedestrian trajectory prediction framework for automated vehicles," *Transportation Research Part C: Emerging Technologies*, vol. 134, January 2022.
- [27] C. Zhang, A. H. Kalantari, Y. Yang, Z. Ni, G. Markkula, N. Merat, and C. Berger, "Cross or wait? Predicting pedestrian interaction outcomes at unsignalized crossings," in *2023 IEEE Intelligent Vehicles Symposium (IV)*. IEEE, 2023, pp. 1–8.
- [28] H. Zhang, Y. Liu, C. Wang, R. Fu, Q. Sun, and Z. Li, "Research on a pedestrian crossing intention recognition model based on natural observation data," *Sensors*, vol. 20, no. 6, p. 1776, 2020.
- [29] W. Zhan, L. Sun, D. Wang, H. Shi, A. Clausse, M. Naumann, J. Kümmerle, H. Königshof, C. Stiller, A. de La Fortelle, and M. Tomizuka, "INTERACTION dataset: An international, adversarial and cooperative motion dataset in interactive driving scenarios with semantic maps," arXiv:1910.03088 [cs, eess], Sep. 2019.
- [30] S. Ettinger, S. Cheng, B. Caine, C. Liu, H. Zhao, S. Pradhan, Y. Chai, B. Sapp, C. R. Qi, Y. Zhou et al., "Large scale interactive motion forecasting for autonomous driving: The waymo open motion dataset," in *Proceedings of the IEEE/CVF international conference on computer vision*, 2021, pp. 9710–9719.
- [31] H. Caesar, V. Bankiti, A. H. Lang, S. Vora, V. E. Liong, Q. Xu, A. Krishnan, Y. Pan, G. Baldan, and O. Beijbom, "nusenes: A multimodal dataset for autonomous driving," in *Proceedings of the IEEE/CVF conference on computer vision and pattern recognition*, 2020, pp. 11 621–11 631.
- [32] A. Rasouli, I. Kotseruba, T. Kunic, and J. K. Tsotsos, "PIE: A large-scale dataset and models for pedestrian intention estimation and trajectory prediction," in *International Conference on Computer Vision (ICCV)*, 2019.
- [33] F. Pascucci, N. Rinke, C. Schiermeyer, V. Berkahn, and B. Friedrich, "A discrete choice model for solving conflict situations between pedestrians and vehicles in shared space," Sep. 2017.
- [34] W. Zhou, J. S. Berrio, C. De Alvis, M. Shan, S. Worrall, J. Ward, and E. Nebot, "Developing and testing robust autonomy: The university of sydney campus data set," *IEEE Intelligent Transportation Systems Magazine*, vol. 12, no. 4, pp. 23–40, 2020.
- [35] M. L. Walters, K. Dautenhahn, S. N. Woods, and K. L. Koay, "Robotic etiquette: Results from user studies involving a fetch and carry task," in *Proceedings of the ACM/IEEE international conference on Human-robot interaction*, 2007, pp. 317–324.
- [36] A. Garrell, M. Villamizar, F. Moreno-Noguer, and A. Sanfeliu, "Proactive behavior of an autonomous mobile robot for human-assisted learning," in *2013 IEEE RO-MAN*. IEEE, 2013, pp. 107–113.
- [37] M. Prédhumeau, A. Spalanzani, and J. Dugdale, "Pedestrian behavior in shared spaces with autonomous vehicles: An integrated framework and review," *IEEE Transactions on Intelligent Vehicles*, vol. 8, no. 1, January 2023.
- [38] J. P. Nuñez Velasco, H. Farah, B. van Arem, and M. P. Hagenzieker, "Studying pedestrians' crossing behavior when interacting with automated vehicles using virtual reality," *Transportation Research Part F: Traffic Psychology and Behaviour*, vol. 66, October 2019.
- [39] S. Hochreiter and J. Schmidhuber, "Long short-term memory," *Neural computation*, vol. 9, no. 8, pp. 1735–1780, 1997.
- [40] S. Hossain, F. T. Johora, J. P. Müller, and S. Hartmann, "A conceptual model of conflicts in shared spaces," in *Proceedings of the 6th International Conference on Industrial and Business Engineering*, 2020, pp. 228–235.
- [41] M. Prédhumeau, L. Mancheva, J. Dugdale, and A. Spalanzani, "Agent-based modeling for predicting pedestrian trajectories around an autonomous vehicle," *Journal of Artificial Intelligence Research*, vol. 73, pp. 1385–1433, 2022.
- [42] M. M. Rashid, M. Seyedi, and S. Jung, "Simulation of pedestrian interaction with autonomous vehicles via social force model," *Simulation modelling practice and theory*, vol. 132, p. 102901, 2024.
- [43] C. Anderson, R. Vasudevan, and M. Johnson-Roberson, "Off the beaten sidewalk: Pedestrian prediction in shared spaces for autonomous vehicles," *IEEE Robotics and Automation Letters*, vol. 5, no. 4, pp. 6892–6899, Oct. 2020.
- [44] E. P. Kampitakis, P. Fafoutellis, G.-M. Oprea, and E. I. Vlahogianni, "Shared space multi-modal traffic modeling using lstm networks with repulsion map and an intention-based multi-loss function," *Transportation Research Part C: Emerging Technologies*, vol. 150, p. 104104, 2023.
- [45] H. Cheng and M. Sester, "Modeling mixed traffic in shared space using LSTM with probability density mapping," in *2018 21st International Conference on Intelligent Transportation Systems (ITSC)*. IEEE, 2018, pp. 3898–3904.

- [46] P. Fafoutellis, E. P. Kampitakis, and E. I. Vlahogianni, "A deep learning framework for modeling pedestrian-vehicle interactions in shared space," in *2023 8th International Conference on Models and Technologies for Intelligent Transportation Systems (MT-ITS)*. IEEE, 2023, pp. 1–6.
- [47] B. Yang, S. Yan, Z. Wang, and K. Nakano, "Prediction based trajectory planning for safe interactions between autonomous vehicles and moving pedestrians in shared spaces," *IEEE Transactions on Intelligent Transportation Systems*, vol. 24, no. 10, pp. 10513–10524, 2023.
- [48] F. T. Johora, H. Cheng, J. P. Müller, and M. Sester, "An agent-based model for trajectory modelling in shared spaces: A combination of expert-based and deep learning approaches," in *Proceedings of the 19th International Conference on Autonomous Agents and MultiAgent Systems*, 2020, pp. 1878–1880.
- [49] G. Yang, E. J. L. Pulgarin, and G. Herrmann, "A hierarchical forecasting model of pedestrian crossing behavior for autonomous vehicle," *IEEE Access*, vol. 12, pp. 9025–9037, 2024.
- [50] I. B. Adhanom, P. MacNeillage, and E. Folmer, "Eye tracking in virtual reality: A broad review of applications and challenges," *Virtual Reality*, vol. 27, no. 2, pp. 1481–1505, 2023.
- [51] S. Bhandari, P. Lencastre, R. Mathema, A. Szorkovszky, A. Yazidi, and P. G. Lind, "Modeling eye gaze velocity trajectories using GANs with spectral loss for enhanced fidelity," *Scientific Reports*, vol. 15, no. 1, p. 19929, 2025.
- [52] A. S. Chan, T.-L. Lee, S. L. Sze, N. S. Yang, and Y. M. Han, "Eye-tracking training improves the learning and memory of children with learning difficulty," *Scientific Reports*, vol. 12, no. 1, p. 13974, 2022.
- [53] T. Chen, P. Samaranyake, X. Cen, M. Qi, and Y.-C. Lan, "The impact of online reviews on consumers' purchasing decisions: Evidence from an eye-tracking study," *Frontiers in Psychology*, vol. 13, p. 865702, 2022.
- [54] S. C. Boerman and C. M. Müller, "Understanding which cues people use to identify influencer marketing on instagram: An eye tracking study and experiment," *International Journal of Advertising*, vol. 41, no. 1, pp. 6–29, 2022.
- [55] Z. Liu, Z. Yang, Y. Gu, H. Liu, and P. Wang, "The effectiveness of eye tracking in the diagnosis of cognitive disorders: A systematic review and meta-analysis," *PloS one*, vol. 16, no. 7, p. e0254059, 2021.
- [56] K. Kim, Y. K. Lee, H. Ahn, S. Hahn, and S. Oh, "Pedestrian intention prediction for autonomous driving using a multiple stakeholder perspective model," in *2020 IEEE/RSJ International Conference on Intelligent Robots and Systems (IROS)*, Oct. 2020, pp. 7957–7962.
- [57] M. Lanzer, I. Koniakowsky, M. Colley, and M. Baumann, "Interaction effects of pedestrian behavior, smartphone distraction and external communication of automated vehicles on crossing and gaze behavior," in *Proceedings of the 2023 CHI Conference on Human Factors in Computing Systems*, April 2023.
- [58] J. Bindschädel, I. Krems, and A. Kiesel, "Two-step communication for the interaction between automated vehicles and pedestrians," *Transportation Research Part F: Traffic Psychology and Behaviour*, vol. 90, 2022.
- [59] J. Bindschädel, I. Krems, and A. Kiesel, "Active vehicle pitch motion for communication in automated driving," *Transportation Research Part F: Traffic Psychology and Behaviour*, vol. 87, May 2022.
- [60] H. Tapiro, T. Oron-Gilad, and Y. Parmet, "Cell phone conversations and child pedestrian's crossing behavior: A simulator study," *Safety Science*, vol. 89, November 2016.
- [61] —, "Pedestrian distraction: the effects of road environment complexity and age on pedestrian's visual attention and crossing behavior," *Journal of Safety Research*, vol. 72, February 2020.
- [62] M. Lanzer and M. Baumann, "Does crossing the road in a group influence pedestrians' gaze behavior?" *Proceedings of the Human Factors and Ergonomics Society Annual Meeting*, vol. 64, no. 1, December 2020.
- [63] A. Sobhani and B. Farooq, "Impact of smartphone distraction on pedestrians' crossing behaviour: An application of head-mounted immersive virtual reality," *Transportation Research Part F: Traffic Psychology and Behaviour*, vol. 58, October 2018.
- [64] G. Bremer and M. Lappe, "Predicting locomotion intention using eye movements and EEG with LSTM and Transformers," in *2024 IEEE International Symposium on Mixed and Augmented Reality (ISMAR)*, Oct. 2024, pp. 21–30.
- [65] G. Bremer, N. Stein, and M. Lappe, "Predicting future position from natural walking and eye movements with machine learning," in *2021 IEEE international conference on artificial intelligence and virtual reality (AIVR)*. IEEE, 2021, pp. 19–28.
- [66] N. Stein, G. Bremer, and M. Lappe, "Eye tracking-based LSTM for locomotion prediction in VR," in *2022 IEEE conference on virtual reality and 3D user interfaces (VR)*. IEEE, 2022, pp. 493–503.
- [67] Y. Kim, S. Hwang, J. Oh, and S. Kim, "Gaitway: Gait data-based VR locomotion prediction system robust to visual distraction," in *Extended Abstracts of the CHI Conference on Human Factors in Computing Systems*, 2024, pp. 1–8.
- [68] S.-B. Jeon, J. Jung, J. Park, and I.-K. Lee, "F-RDW: Redirected walking with forecasting future position," *IEEE Transactions on Visualization and Computer Graphics*, vol. 31, no. 4, pp. 1970–1984, Apr. 2025.
- [69] Y. Feng, H. Farah, and B. van Areem, "Effect of ehmi on pedestrian road crossing behavior in shared space with automated vehicles—a virtual reality study," in *2023 IEEE 26th International Conference on Intelligent Transportation Systems (ITSC)*. IEEE, 2023, pp. 2038–2043.
- [70] S. M. Faas, L.-A. Mathis, and M. Baumann, "External hmi for self-driving vehicles: Which information shall be displayed?" *Transportation research part F: traffic psychology and behaviour*, vol. 68, pp. 171–186, 2020.
- [71] A. Rasouli and J. K. Tsotsos, "Autonomous vehicles that interact with pedestrians: A survey of theory and practice," *IEEE Transactions on Intelligent Transportation Systems*, vol. 21, no. 3, pp. 900–918, Mar. 2020.
- [72] M. D. McKay, R. J. Beckman, and W. J. Conover, "A comparison of three methods for selecting values of input variables in the analysis of output from a computer code," *Technometrics*, 1979.
- [73] R. S. Kennedy, N. E. Lane, K. S. Berbaum, and M. G. Lilienthal, "Simulator sickness questionnaire: An enhanced method for quantifying simulator sickness," *The International Journal of Aviation Psychology*, vol. 3, no. 3, pp. 203–220, Jul. 1993.
- [74] B. G. Witmer, C. J. Jerome, and M. J. Singer, "The factor structure of the presence questionnaire," *Presence: Teleoperators and Virtual Environments*, vol. 14, no. 3, pp. 298–312, Jun. 2005.
- [75] S. Deb, L. Strawderman, D. W. Carruth, J. DuBien, B. Smith, and T. M. Garrison, "Development and validation of a questionnaire to assess pedestrian receptivity toward fully autonomous vehicles," *Transportation Research Part C: Emerging Technologies*, Nov. 2017.
- [76] W. Payre, J. Cestac, and P. Delhomme, "Fully automated driving: Impact of trust and practice on manual control recovery," *Human Factors*, vol. 58, no. 2, pp. 229–241, Mar. 2016.
- [77] J. Bindschädel, I. Krems, and A. Kiesel, "Interaction between pedestrians and automated vehicles: Exploring a motion-based approach for virtual reality experiments," *Transportation Research Part F: Traffic Psychology and Behaviour*, vol. 82, pp. 316–332, 2021.
- [78] J. W. Grootjen, H. Weingärtner, and S. Mayer, "Uncovering and addressing blink-related challenges in using eye tracking for interactive systems," in *Proceedings of the 2024 CHI Conference on Human Factors in Computing Systems*, ser. CHI '24. New York, NY, USA: Association for Computing Machinery, May 2024, pp. 1–23.
- [79] D. D. Salvucci and J. H. Goldberg, "Identifying fixations and saccades in eye-tracking protocols," in *Proceedings of the 2000 symposium on Eye tracking research & applications*, 2000, pp. 71–78.
- [80] H. R. Schiffman, *Sensation and perception: An integrated approach*. John Wiley & Sons, 1990.
- [81] S. M. Lundberg and S.-I. Lee, "A unified approach to interpreting model predictions," *Advances in neural information processing systems*, vol. 30, 2017.
- [82] E. Postuma, F. Cornelissen, M. Pahlevan, J. Heutink, and G. de Haan, "Reduced field of view alters scanning behaviour," *Virtual Reality*, vol. 29, no. 2, pp. 1–17, 2025.
- [83] L. Kooijman, R. Happee, and J. C. de Winter, "How do ehmis affect pedestrians' crossing behavior? a study using a head-mounted display combined with a motion suit," *Information*, vol. 10, no. 12, p. 386, 2019.
- [84] D. Dey, K. Holländer, M. Berger, B. Eggen, M. Martens, B. Pflöging, and J. Terken, "Distance-dependent ehmis for the interaction between automated vehicles and pedestrians," in *12th international conference on automotive user interfaces and interactive vehicular applications*, 2020, pp. 192–204.
- [85] J. Zębala, P. Ciepka, and A. Reza, "Pedestrian acceleration and speeds," *Problems of Forensic Sciences*, vol. 91, pp. 227–234, 2012.
- [86] N. Misdariis, A. Gruson, and P. Susini, "Detectability study of warning signals in urban background noises: A first step for designing the sound of electric vehicles," *Proceedings of Meetings on Acoustics*, vol. 19, no. 1, p. 040032, May 2013.
- [87] D. S. Kim, R. W. Emerson, K. Naghshineh, J. Pliskow, and K. Myers, "Impact of adding artificially generated alert sound to hybrid electric vehicles on their detectability by pedestrians who are blind," *Journal of Rehabilitation Research and Development*, vol. 49, no. 3, pp. 381–394, May 2012.
- [88] I. Salleh, M. Z. M. Zain, and R. I. R. Hamzah, "Evaluation of annoyance and suitability of a back-up warning sound for electric vehicles," *International Journal of Automotive and Mechanical Engineering*, vol. 8, pp. 1267–1277, 2013.

- [89] J.-F. Petiot, K. Legeay, and M. Lagrange, "Optimization of the sound of electric vehicles according to unpleasantness and detectability," *ResearchGate*, Aug. 2019.
- [90] U. Sandberg, L. Goubert, and P. Mioduszewski, "Are vehicles driven in electric mode so quiet that they need acoustic warning signals," in *20th International Congress on Acoustics*. sn, 2010.
- [91] T. Akiba, S. Sano, T. Yanase, T. Ohta, and M. Koyama, "Optuna: A next-generation hyperparameter optimization framework," in *Proceedings of the 25th ACM SIGKDD International Conference on Knowledge Discovery and Data Mining*, 2019.

APPENDICES

A. Details of experiment setup

1) *Calculation of shuttles' initial distance:* The process was split into two stages: (1) the pedestrian stood still, then accelerated, and maintained their speed until the decision point, and (2) the pedestrian decided whether to cross or not face the situation. So, for stage (1), it took the same time for pedestrians and shuttles to arrive at the blue point. For stage (2), the pedestrian had 1.5 meters to react, and the shuttle had a critical gap equal to 2.5 seconds. This resulted in a starting distance of the shuttle of 17.3 meters. The shuttle size is 3 meters \times 1.6 meters. Pedestrian average walking speed is 1.3 meters/second, and average acceleration is 1 meter/second [85]. An illustration is shown in Fig. 8.

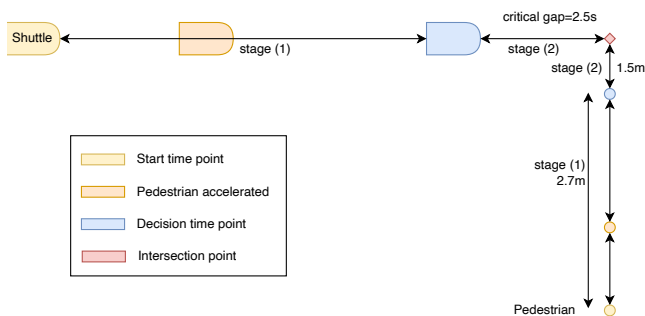


Fig. 8. An illustration of the design of interactions.

2) *Calculation of eHMI activation point:* We activated eHMI when it was 2.5 seconds away from the pedestrian's final decision-making point. In other words, a red pedestrian eHMI sign appeared starting from 10.42 meters ($=15\text{km/h} / 0.036 * 2.5$ seconds); a green pedestrian eHMI sign appeared starting from 7.96 meters (as shown in the deceleration profile: when the shuttle was 7.96 meters away from the pedestrian, it needed 2.5 seconds to stop).

3) *Sound design:* To ensure realism and immersion, there was audio in each scenario. Background ambient noise was used to simulate an outdoor shared space, and audio clips were used for the pod operating. The background sound is around 56 decibels [86]. Vehicles approaching about 15 km/h were detected at 27 meters for hybrids in electric mode [87] and reached about 55 decibels at 2 meters [88]. To simplify the vehicle's sound effect implementation, we assumed the influence from distance and speed only. For distance, we adopted the sound level inversely proportional to the distance to the listener [89]. For speed, there is a log relationship between sound level and vehicle speed [90]. The sound was

displayed with spatial effects in the virtual environment, but it was not possible to distinguish sounds from more than two shuttles except by using distance cues. As Unreal Engine 5 was hard to achieve specific decibels, we conducted a pilot study to decide which sound level can realistically reflect the real-world sound effect.

B. Implementation details

The hyperparameters of all models were tuned using the Optuna framework [91] on our dataset to make a fair comparison. All models were tuned over 150 trials for the best hyperparameters, and each trial runs 100 epochs. The learning rate decay is the same, which uses [15, 35, 60] as milestones, and the decay rate is 0.2. The optimizer is the Adam optimizer. The prediction is on the delta movement.